

76-56
ADA 031208
AFFDL-TR-76-56

PREDICTION OF THE ANGULAR VIBRATION OF AIRCRAFT STRUCTURES

LOAN COPY
*AEROSPACE DYNAMICS BRANCH
STRUCTURES DIVISION*

JUNE 1976

TECHNICAL REPORT AFFDL-TR-76-56
FINAL REPORT FOR PERIOD SEPTEMBER 1975 - JANUARY 1976

Approved for public release; distribution unlimited

AIR FORCE FLIGHT DYNAMICS LABORATORY
AIR FORCE WRIGHT AERONAUTICAL LABORATORIES
AIR FORCE SYSTEMS COMMAND
WRIGHT-PATTERSON AIR FORCE BASE, OHIO 45433

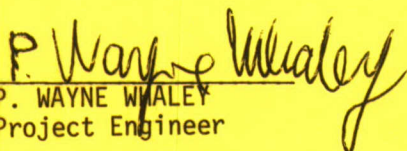
20080815 146

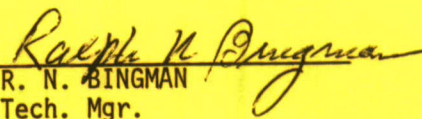
NOTICE

When Government drawings, specifications, or other data are used for any purpose other than in connection with a definitely related Government procurement operation, the United States Government thereby incurs no responsibility nor any obligation whatsoever; and the fact that the government may have formulated, furnished, or in any way supplied the said drawings, specifications, or other data, is not to be regarded by implication or otherwise as in any manner licensing the holder or any other person or corporation, or conveying any rights or permission to manufacture, use, or sell any patented invention that may in any way be related thereto.

This report has been reviewed by the Information Office (OI) and is releasable to the National Technical Information Service (NTIS). At NTIS, it will be available to the general public, including foreign nations.

This technical report has been reviewed and is approved for publication.


P. WAYNE WHALEY
Project Engineer


R. N. BINGMAN
Tech. Mgr.

FOR THE COMMANDER


HOLLAND B. LOWNDES, JR.
Chief, Structural Mechanics Division

Copies of this report should not be returned unless return is required by security considerations, contractual obligations, or notice on a specific document.

UNCLASSIFIED

SECURITY CLASSIFICATION OF THIS PAGE (When Data Entered)

REPORT DOCUMENTATION PAGE		READ INSTRUCTIONS BEFORE COMPLETING FORM
1. REPORT NUMBER AFFDL-TR-76-56	2. GOVT ACCESSION NO.	3. RECIPIENT'S CATALOG NUMBER
4. TITLE (and Subtitle) PREDICTION OF THE ANGULAR VIBRATION OF AIRCRAFT STRUCTURES		5. TYPE OF REPORT & PERIOD COVERED Final Report September 75 - January 76
		6. PERFORMING ORG. REPORT NUMBER
7. AUTHOR(s) Jon Lee P. Wayne Whaley		8. CONTRACT OR GRANT NUMBER(s)
9. PERFORMING ORGANIZATION NAME AND ADDRESS Aerospace Dynamics Branch (FBD) Air Force Flight Dynamics Laboratory Wright-Patterson Air Force Base, Ohio 45433		10. PROGRAM ELEMENT, PROJECT, TASK AREA & WORK UNIT NUMBERS 13700218
11. CONTROLLING OFFICE NAME AND ADDRESS Air Force Flight Dynamics Laboratory Wright-Patterson Air Force Base, Ohio 45433		12. REPORT DATE June 1976
		13. NUMBER OF PAGES 35
14. MONITORING AGENCY NAME & ADDRESS (if different from Controlling Office)		15. SECURITY CLASS. (of this report) UNCLASSIFIED
		15a. DECLASSIFICATION/DOWNGRADING SCHEDULE
16. DISTRIBUTION STATEMENT (of this Report) Approved for public release; distribution unlimited.		
17. DISTRIBUTION STATEMENT (of the abstract entered in Block 20, if different from Report)		
18. SUPPLEMENTARY NOTES Presented at the AIAA-AFWAL Mini-Symposium, Air Force Institute of Technology, 25 March 1976.		
19. KEY WORDS (Continue on reverse side if necessary and identify by block number) Angular Vibration Prediction, Aircraft Angular Vibration, Random Vibration, Forced Vibration, Angular Motion		
20. ABSTRACT (Continue on reverse side if necessary and identify by block number) Using the Bernoulli-Euler beam as a theoretical model, qualitative relationships have been developed to predict the angular vibration from a prescribed linear vibration response. Based on laboratory and flight test data, the overall accuracy of predictions is within $\pm 20\%$ of the angular vibration measurements. Such a prediction capability may be considered very significant in that the prediction schemes are intended only for qualitative purposes. In addition, due to the difficulties in obtaining accurate angular measurements, the present vibration data are limited to a gross confirmation of predictions.		

FOREWORD

This work was performed by personnel of the Aerospace Dynamics Branch, Structures Division, Air Force Flight Dynamics Laboratory (AFFDL/FBD), Wright-Patterson Air Force Base, Ohio. This study was conducted in support of Project 1370, "Dynamic Problems in Flight Vehicles," Task 137002, "Flight Vehicle Vibration Control," Work Unit 13700218, "Aircraft Linear and Angular Vibration Prediction."

The research described in this report was conducted by P. Wayne Whaley, Principal investigator, and by Dr. Jon Lee over the period of September 1975 through January 1976.

This report was submitted by the authors during February 1976.

ADA031208

TABLE OF CONTENTS

SECTION	PAGE
I INTRODUCTION	1
II THEORETICAL ANALYSIS	3
1. Linear and Angular Deflections	4
2. Vibration Amplitude	5
3. Random Forcing $q(x)$	7
4. Localized Forcing $q(x)$	8
III THE BEAM-AVERAGED VIBRATION RMS AMPLITUDE	10
IV THE DISCRETE ANGLE	15
V PRACTICAL DEFINITION OF THE DISCRETE ANGULAR VIBRATION	19
VI CONCLUSIONS	23
APPENDIX STOCHASTIC ANALYSIS OF THE TIMOSHENKO BEAM	24
REFERENCES	26

LIST OF ILLUSTRATIONS

FIGURE	PAGE
1. Simply Supported Beam	3
2. PSD of Transverse Vibration	13
3. PSD of Angular Vibration	14
4. Correlation Coefficient	22

LIST OF TABLES

TABLE	PAGE
1. Relative Magnitudes of the Lower-Order I_{nk}	9
2. Comparison of the Measured and Predicted $(\Delta y / \Delta x)_{rms}$	18

LIST OF SYMBOLS

A	Numerical factor of Equation 27
E	Modulus of elasticity
$F_g(\omega)$	Psd of $g(t)$
$f(x,t)$	Excitation/mass
$g(t)$	Temporal part of $f(x,t)$
$H_n(t)$	Modal frequency-response
$h_n(t)$	Modal impulse-response
I	Moment of inertia
I_{nk}	Integral defined by Equation 11
L	Beam length
m	Mass/length
$q(x)$	Spatial part of $f(x,t)$
q_n	Modal forcing
$R_g(t)$	Temporal correlation of $g(t)$
$R_q(x,y)$	Spatial correlation of $q(x)$ and $q(y)$
t	Time
x	Length-wise coordinate
Δx	Separation distance
$y(x,t)$	Transverse displacement
y_n	Modal displacement
$\Delta y/\Delta x$	Discrete angle defined by Equation 28
$< >$	Statistical average

LIST OF SYMBOLS (CONTINUED)

GREEKS

β	Damping constant
η	Correlation coefficient
δ_{nk}	Kronecker delta
$\delta(x)$	Dirac delta function
$\theta(x,t)$	$dy(x,t)/dx$
τ	Difference time
ω	Angular frequency (Rad/sec)

$$\omega_n \quad \left(\frac{n\pi}{L} \right)^2 \sqrt{\frac{EI}{m}}$$

$$\omega'_n \quad \sqrt{\omega_n^2 - \beta^2}$$

Subscript

$()_{rms}$	Beam-averaged rms defined by
-------------	------------------------------

$$\sqrt{L^{-1} \int_0^L < ()^2 > dx}$$

SECTION I

INTRODUCTION

The performance of airborne electrooptical systems may be seriously affected by the angular as well as the linear vibration. Unlike the linear vibration, very little experimental data are available for the angular vibration. The purpose of this report is to investigate the relationship between the linear and angular structural vibration characteristics thereby developing prediction schemes for the angular vibration amplitude from a prescribed linear vibration environment. Precisely speaking, the linear vibration refers to the transverse deflection, whereas the angular vibration is due to the rotary mode of internal bending, the effect of which is included in the Timoshenko beam equation (Reference 1). For a small amplitude vibration, the angular (rotary) deflection can be related to the slope of the linear (transverse) displacement. This provides a theoretical basis for relating the linear and angular vibrations.

As a theoretical model, Section II considers the Bernoulli-Euler beam with simply supported ends and formulates the stochastic dynamics for the linear and angular deflections. For maximal simplicity, an idealized random forcing function is imposed to generate the stationary response dynamics. Since the stochastic beam analysis has already been presented (References 2 and 3), only the main steps of analysis which yield the linear and angular variances as infinite series will be summarized. It is important to note that the response variance has the same form for both the beam and plate problems when the normal-mode representation is used. This is why a beam analysis can provide the basic relationship of stochastic dynamics which is also valid for the plate structure. To be realistic, the aircraft fuselage must be modeled by a stringer stiffened cylindrical shell. Since such a model is not amenable to qualitative analysis, an alternate approach would be to build up the aircraft fuselage by piece-wise flat panels joined together by stiffeners. The motivation for the present analysis is that a beam/plate model can describe certain essential features of aircraft fuselage vibration in a qualitative manner.

In Section III, an attempt is made to derive a qualitative relationship between the linear and angular rms amplitudes, which is valid for the general vibration environment. This has been accomplished by averaging the linear and angular variances over the beam, thereby integrating away the normal modes on which the analysis of Section II is based. By truncating the variances to lowest orders, a simple prediction (Equation 27) has been obtained to relate the beam-averaged linear and angular rms amplitudes. However, due to the scarcity of angular vibration data, comparisons of predicted and measured angular vibration are necessarily quite limited.

Because of the difficulties associated with many angular vibration measurement techniques, a practical approach is to calculate a discrete angle by differencing two linear accelerometer signals and then dividing by the separation distance. The main goal of Section IV is to provide a prediction for the discrete angular vibration. Based on some laboratory test data, the accuracy of the prediction scheme as given by Equation 33 is about $\pm 20\%$ of the measured angular vibration. Although quite crude, it bolsters one's confidence in that the prediction scheme is intended for qualitative purposes and the present vibration data are limited only to a gross confirmation of predictions.

The discrete angle defined by the difference of two linear accelerometer signals is not well suited for statistical analyses, especially when the separation distance becomes small. This is because the differencing operation tends to accentuate the noise part of random signals. Consequently, the smaller the separation distance, the more acute the differencing error. In Section V an alternate definition is presented of the discrete angular vibration which involves the difference of elements of the covariance matrix and not the random signals themselves. Surprisingly, such a definition of the angular motion has not yet been explored. Its practical implication is being investigated and will be discussed in a later report.

SECTION II

THEORETICAL ANALYSIS

The transverse deflection of a Bernoulli-Euler beam (Figure 1) is governed by the equation

$$\frac{\partial^2 y}{\partial t^2} + 2\beta \frac{\partial y}{\partial t} + \frac{EI}{m} \frac{\partial^4 y}{\partial x^4} = f(x,t), \quad (1)$$

where EI is the flexural rigidity, m is the mass/unit length of the prismatic beam, β is the damping constant, and $f(x,t)$ is the excitation/mass. It will be assumed that the forcing function splits into the spatial part ($q(x)$) and the temporal part ($g(t)$)

$$f(x,t) = q(x) g(t).$$

As pointed out in the Introduction, the Timoshenko beam incorporates the angular effect of internal bending, whereas the Bernoulli-Euler beam does not. Therefore, it might appear that the use of Equation 1 is not appropriate for angular vibration work. As shown in the Appendix, however, both beam theories give the same prediction scheme; hence it is more economical to base the analysis on Equation 1, which is somewhat simpler than the Timoshenko beam equation. The stochastic dynamics of Equation 1 have already been investigated by Eringen (Reference 2), and Bogdanoff and Goldberg (Reference 3), so that it suffices to outline only the main steps.

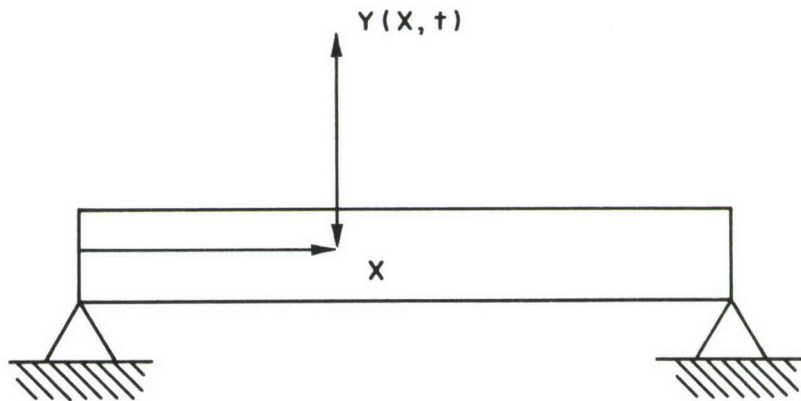


Figure 1. Simply Supported Beam

1. LINEAR AND ANGULAR DEFLECTIONS

For the simply supported beam of length L , the undamped normal mode $\sin(n\pi x/L)$ can be used to express the spatial behavior

$$y(x,t) = \sum_{n=1}^{\infty} y_n(t) \sin\left(\frac{n\pi x}{L}\right) \quad (2a)$$

$$q(x) = \sum_{n=1}^{\infty} q_n \sin\left(\frac{n\pi x}{L}\right) \quad (2b)$$

The insertion of Equation 2 into Equation 1 gives

$$\ddot{y}_n + 2\beta \dot{y}_n + \omega_n^2 y_n = q_n g(t),$$

where the dot denotes $\partial/\partial t$, and $\omega_n^2 = (n\pi/L)^4 EI/m$. The particular solution with zero initial conditions is

$$y_n(t) = q_n \int_0^t h_n(t-\tau) g(\tau) d\tau. \quad (3)$$

Here the impulse-response function is given by

$$h_n(t) = \frac{\exp(-\beta t)}{\omega_n} \sin \omega_n' t \quad (4)$$

where $\omega_n' = \sqrt{\omega_n^2 - \beta^2}$. By letting $t_0 \rightarrow -\infty$, one may rewrite Equation 3 as

$$y_n(t) = q_n \int_0^{\infty} h_n(\tau) g(t-\tau) d\tau \quad (5)$$

The introduction of Equation 5 into Equation 2a would then yield the linear deflection

$$y(x,t) = \sum_{n=1}^{\infty} \sin\left(\frac{n\pi x}{L}\right) q_n \int_0^{\infty} h_n(\tau) g(t-\tau) d\tau, \quad (6)$$

subject to the arbitrary forcing. For a small amplitude vibration, the angular deflection $\theta(x,t)$ is approximated by the derivative $dy(x,t)/dx$,

$$\theta(x,t) = \sum_{n=1}^{\infty} \left(\frac{n\pi}{L} \right) \cos \left(\frac{n\pi x}{L} \right) q_n \int_0^{\infty} h_n(\tau) g(t-\tau) d\tau \quad (7)$$

Thus, the linear and angular deflections are formally expressed by Equations 6 and 7 respectively.

2. VIBRATION AMPLITUDE

When the forcing function is random, so are the linear and angular deflections. Let us therefore compute the variance of $y(x,t)$

$$\begin{aligned} \langle y^2(x,t) \rangle &= \sum_{n,k} \sin \left(\frac{n\pi x}{L} \right) \sin \left(\frac{k\pi x}{L} \right) \langle q_n q_k \rangle \\ &\int_0^{\infty} \int_0^{\infty} h_n(\tau_1) h_k(\tau_2) \langle g(t-\tau_1) g(t-\tau_2) \rangle d\tau_1 d\tau_2, \end{aligned} \quad (8)$$

where $\langle \rangle$ denotes statistical average or expectation. It must be pointed out that the statistical independence of $q(x)$ and $g(t)$ has been invoked in Equation 8, which greatly simplifies the subsequent analysis. For instance, this assumption cannot be applied when a beam or plate is excited by convecting turbulent pressure fluctuations (References 4 and 5). For stationary random forcing, the correlation $\langle g(t-\tau_1) g(t-\tau_2) \rangle$ is a function of the time difference $\tau = \tau_2 - \tau_1$. By the Wiener-Khinchin theorem (Reference 6), the stationary correlation of the forcing function denoted by $R_g(\tau)$ is related to the power spectral density (psd) denoted by $F_g(\omega)$.

$$\begin{aligned} R_g(\tau) &= \frac{1}{2} \int_{-\infty}^{\infty} F_g(\omega) \exp(i\omega\tau) d\omega, \\ F_g(\omega) &= (1/\pi) \int_{-\infty}^{\infty} R_g(\tau) \exp(-i\omega\tau) d\tau. \end{aligned} \quad (9)$$

Under the stationary forcing, it is evident that Equation 8 is independent of t , hence

$$\langle y^2(x) \rangle = \sum_{n,k} \sin\left(\frac{n\pi x}{L}\right) \sin\left(\frac{k\pi x}{L}\right) \langle q_n q_k \rangle I_{nk}, \quad (10)$$

where

$$I_{nk} = \frac{1}{2} \int_{-\infty}^{\infty} d\omega F_g(\omega) \int_0^{\infty} h_n(\tau_1) e^{-i\omega\tau_1} d\tau_1 \int_0^{\infty} h_k(\tau_2) e^{i\omega\tau_2} d\tau_2. \quad (11)$$

Similarly, the stationary angular variance is given by

$$\langle \theta^2(x) \rangle = \left(\frac{\pi}{L}\right)^2 \sum_{n,k} nk \cos\left(\frac{n\pi x}{L}\right) \cos\left(\frac{k\pi x}{L}\right) \langle q_n q_k \rangle I_{nk} \quad (12)$$

With the use of Equation 4, one finds by a simple computation that

$$\int_0^{\infty} h_n(\tau_1) \exp(-i\omega\tau_1) d\tau_1 = \frac{1}{\omega_n^2 + 2i\beta\omega - \omega^2} = H_n(\omega),$$

which is the frequency-response function. Hence, Equation 11 may be put in the compact form

$$I_{nk} = \frac{1}{2} \int_{-\infty}^{\infty} F_g(\omega) H_n(\omega) H_k^*(\omega) d\omega, \quad (13)$$

where $*$ denotes the complex conjugate. When the normal-mode representation is used (Reference 2), the form of linear and angular variances is the same for both the beam and plate problems in that it consists of the normal modes, the spatial correlation $\langle q_n q_k \rangle$, and the I_{nk} .

To explicitly evaluate Equation 13, one must further specify $F_g(\omega)$. For a typical $R_g(\tau)$ of the exponential form, the corresponding psd has the form

$$F_g(\omega) = \frac{F_0 \omega_0^2}{\omega_0^2 + \omega^2}, \quad (14)$$

where F_0 is a scaling factor, and ω_0 is the relaxation constant. In the limit as $\omega_0 \rightarrow \infty$, Equation 14 reduces to the white-noise spectrum

$$F_g(\omega) = F_0. \quad (15)$$

For simplicity, let us evaluate Equation 13 under the white-noise forcing Equation 15. The result by contour integration is

$$I_{nk} = \frac{4\pi\beta F_0}{(\omega_n^2 - \omega_k^2 - 4\beta^2)^2 + (4\beta\omega_n')^2}, \quad (16)$$

which is $2\pi i$ times the residues at $\omega = i\beta \pm \omega_n'$. For $n = k$, it simplifies to

$$I_{nn} = \frac{\pi F_0}{4\beta\omega_n^2} \quad (17)$$

From the definition of ω_n , it is seen that $I_{nn} \sim 1/n^4$, hence the magnitudes of I_{nn} fall off rapidly with increasing n . Magnitudes of I_{nk} ($n \neq k$) with respect to I_{nn} will be assessed in Section II-4.

3. RANDOM FORCING $q(x)$

In view of Equation 2b, the mean value $\langle q_n q_k \rangle$ has the form

$$\langle q_n q_k \rangle = \frac{2}{L} \int_0^L dx \int_0^L dy R_q(x, y) \sin\left(\frac{n\pi x}{L}\right) \sin\left(\frac{k\pi y}{L}\right), \quad (18)$$

where $R_q(x, y) = \langle q(x)q(y) \rangle$ is the spatial forcing correlation. When spatial homogeneity is assumed, $R_q(x, y)$ is a function of the separation distance only. By letting $z = x - y$, Equation 18 can then be put in the form

$$\langle q_n q_k \rangle = \frac{2}{L} \int_0^L dy \sin\left(\frac{k\pi y}{L}\right) \int_{-\infty}^{\infty} R_q(z) \sin\left(\frac{n\pi(2+y)}{L}\right) dz$$

when $R_q(z)$ is assumed fairly sharp (Reference 7). Now expand $\sin(n\pi(2+y)/L) = \sin(n\pi z/L) \cos(n\pi y/L) + \cos(n\pi z/L) \sin(n\pi y/L)$. Since $R_q(z)$ is even, it is seen that $R_q(z) \sin(n\pi z/L)$ integrates out to zero, and hence Equation 18 becomes

$$\langle q_n q_k \rangle = \delta_{nk} \int_{-\infty}^{\infty} R_q(z) \cos\left(\frac{n\pi z}{L}\right) dz, \quad (19)$$

where the Kronecker $\delta_{nk} = 1$ for $n = k$ and $= 0$ for $n \neq k$. For the infinitely sharp $R_q(z) = K \delta(z)$ (K being a constant), Equation 19 reduces to

$$\langle q_n q_k \rangle = K \delta_{nk} \quad (20)$$

Under the random $q(x)$ with no spatial correlation, the variances shown in Equations 10 and 12 therefore become

$$\langle y^2(x) \rangle = \sum_{n=1}^{\infty} \sin^2 \left(\frac{n\pi x}{L} \right) K I_{nn}, \quad (21a)$$

$$\langle \theta^2(x) \rangle = \left(\frac{\pi}{L} \right)^2 \sum_{n=1}^{\infty} n^2 \cos^2 \left(\frac{n\pi x}{L} \right) K I_{nn}. \quad (21b)$$

Because $I_{nn} \sim n^{-4}$, the series representations are convergent, even though the total power of $f(x,t)$ is infinite. To be more physically realistic, the forcing correlation must exhibit both the spatial and temporal relaxations. Although this can easily be incorporated by Equations 14 and 19, such is not needed for the present purpose.

4. LOCALIZED FORCING $q(x)$

In a laboratory test situation, it is most convenient to apply the external forcing to certain points on a structure. In such a case, the $\langle q_n q_k \rangle$ term is simply a $q_n q_k$. When Equation 20 is not invoked, the variances shown in Equations 10 and 12 are double sums over n and k . For a slightly damped beam it will be shown that I_{nn} are orders of magnitude larger than I_{nk} ($n \neq k$); hence, the variances can still be reduced to a single sum even when $q(x)$ is nonrandom. To this end, some lower-order I_{nk} were computed from Equation 16 with $\beta = \omega_1/10$, and their relative magnitudes have been summarized in Table 1.

TABLE 1
RELATIVE MAGNITUDES OF THE LOWER-ORDER I_{nk}

I_{nk}	I_{11}	I_{22}	I_{33}	$I_{12} \approx I_{21}$	$I_{13} \approx I_{31}$	$I_{32} \approx I_{23}$
Magnitude	1	1/16	1/81	1/1406	1/40375	1/26406

From the table, one may therefore conclude that $I_{nk} \sim n^{-4} \delta_{nk}$ for a slightly damped structure under the white noise excitation.

SECTION III

THE BEAM-AVERAGED VIBRATION RMS AMPLITUDE

Since $I_{nn} \sim n^{-4}$, the first-term approximation of Equation 21a introduces an error on the order of $(1/16)$

$$\langle y^2(x) \rangle = \sin^2 \left(\frac{\pi x}{L} \right) K I_{11}. \quad (22)$$

Because of the factor n^2 , on the other hand, the first-term truncation of Equation 21b

$$\langle \theta^2(x) \rangle = \left(\frac{\pi}{L} \right)^2 \cos^2 \left(\frac{\pi x}{L} \right) K I_{11}, \quad (23)$$

discards a term of the order of $(1/4)$, which is not acceptable. To the same order of approximation as Equation 22, the second and third terms must then be included

$$\langle \theta^2(x) \rangle = \left(\frac{\pi}{L} \right)^2 \sum_{n=1}^3 n^2 \cos^2 \left(\frac{n\pi x}{L} \right) K I_{nn}. \quad (24)$$

For a localized forcing at the mid-span $(L/2)$, $K q_n^2 \sim \sin^2(n\pi/2)$, so that the second term ($n = 2$) will then be absent in Equation 24.

For the overall description, the variances will now be averaged over the beam. First, by applying $L^{-1} \int_0^L dx$ to both sides of Equations 22,

the beam-averaged rms amplitude, $y_{rms} = \sqrt{L^{-1} \int_0^L \langle y^2(x) \rangle dx}$, has the following form

$$y_{rms} = \sqrt{K I_{11}/2}. \quad (25)$$

Next, averaging Equation 24 over the beam in a similar manner, one obtains with the use of $I_{nn} = I_{11}/n^4$

$$\theta_{rms} = \frac{\pi}{L} \sqrt{\frac{K I_{11}}{2} \left(\sum_{n=1}^3 \frac{1}{n^2} \right)^{\frac{1}{2}}}, \quad (26)$$

where $\theta_{rms} = \sqrt{L^{-1} \int_0^L \langle \theta^2(x) \rangle dx}$ is the beam-averaged rms of angular fluctuations. Note that by averaging over the beam we have eliminated the explicit dependence of Equations 22 and 24 on the normal modes, $\sin(n\pi x/L)$, which reflect the simply supported end condition. It is therefore anticipated that Equations 25 and 26 would apply to any beam, at least qualitatively, regardless of the end conditions. The practical implication of beam averaging is that it frees the formulation from a particular end condition. This is important in applications because the boundary (or end) conditions of a structure embedded in airframes cannot be specified precisely. By combining Equations 25 and 26, the main result of this section is

$$\theta_{rms} = A \left(\frac{\pi}{L} \right) y_{rms}, \quad (27)$$

where

$$A = \begin{cases} 1, & \text{for the first-term truncation} \\ & \text{Equation 23} \\ \left(\sum_{n=1}^3 \frac{1}{n^2} \right)^{1/2} \approx 1.17, & \text{for the random } q(x), \\ (1 + 1/8)^{1/2} \approx 1.06, & \text{for the localized } q(x) \text{ at } L/2. \end{cases}$$

Note that only the lowest order modes contribute explicitly to the above relation. Although Equation 27 was obtained from the beam analysis, it should also apply to a plate along the coordinate axes. This is because the basic structure of variance is the same for both the beam and plate problems when the normal-mode representation is used.

Due to the difficulty in angular measurement techniques, angular vibration data are very scarce. Also, it is almost impossible to find a matching set of linear and angular vibration data taken concurrently at the same location on an airframe. Some angular vibration psd have been reported by Sher (Reference 8) during the flight tests of an NC-135 aircraft. Later, Davis (Reference 9) measured the linear vibration psd

on another aircraft of the same type. Apart from the apparent difference in aircraft and flight conditions, it is most unfortunate that the transducer locations of Davis are not the same as those of Sher. In spite of this, an attempt has been made to select a set of linear and angular psd data whose transducer locations are as close as possible. For the present comparison, Figure 30 of Davis (Reference 9) and Figure 8 of Sher (Reference 8) were chosen as a typical set of the linear and angular psd's. They are reproduced here in Figures 2 and 3, respectively. To estimate the rms of vertical displacements, one may approximate the psd of Figure 2 by a power formula of the form, $(5 \times 10^{-5}) \omega^{-2.7}$, which in essence replaces the psd by a straight line in the figure. Then, analytically integrating this power formula over the frequency range of $[2, \infty]$, one obtains $y_{\text{rms}} \approx 3 \times 10^{-3}$ in. Therefore, by treating the entire fuselage as a beam-like structure, $L = 2100$ in., Equation 27 with $A = 1.17$ yields the rms of angular vibration $\theta_{\text{rms}} \approx 5.24 \times 10^{-6}$ rad. Now, to provide an experimental check, θ_{rms} can be estimated directly from Figure 3. Again, for convenience, the psd of Figure 3 may be approximated by a three-piece power formula as depicted in the figure. Then integrating this power formula over the appropriate frequency range, the measured rms of angular vibration is estimated to be $\theta_{\text{rms}} \approx 6.23 \times 10^{-6}$ rad. Although the measured θ_{rms} is almost 20% higher than the predicted, such a comparison is very encouraging in that linear and angular vibration data used here have limited correspondence. The scarcity of vibration data impedes further confirmation of the prediction scheme.¹ Therefore, an alternate prediction will be developed in the next section in terms of the discrete angle, which is readily measurable by the conventional accelerometers.

1. Some additional sets of linear and angular vibration data have been supplied by W. R. Davis, Jr. Although these data seem to support the prediction capability of Equation 27 within $\pm 20\%$, the estimation of rms values from the raw test data involves a number of gross approximations. Hence, the details of comparison will not be presented here.

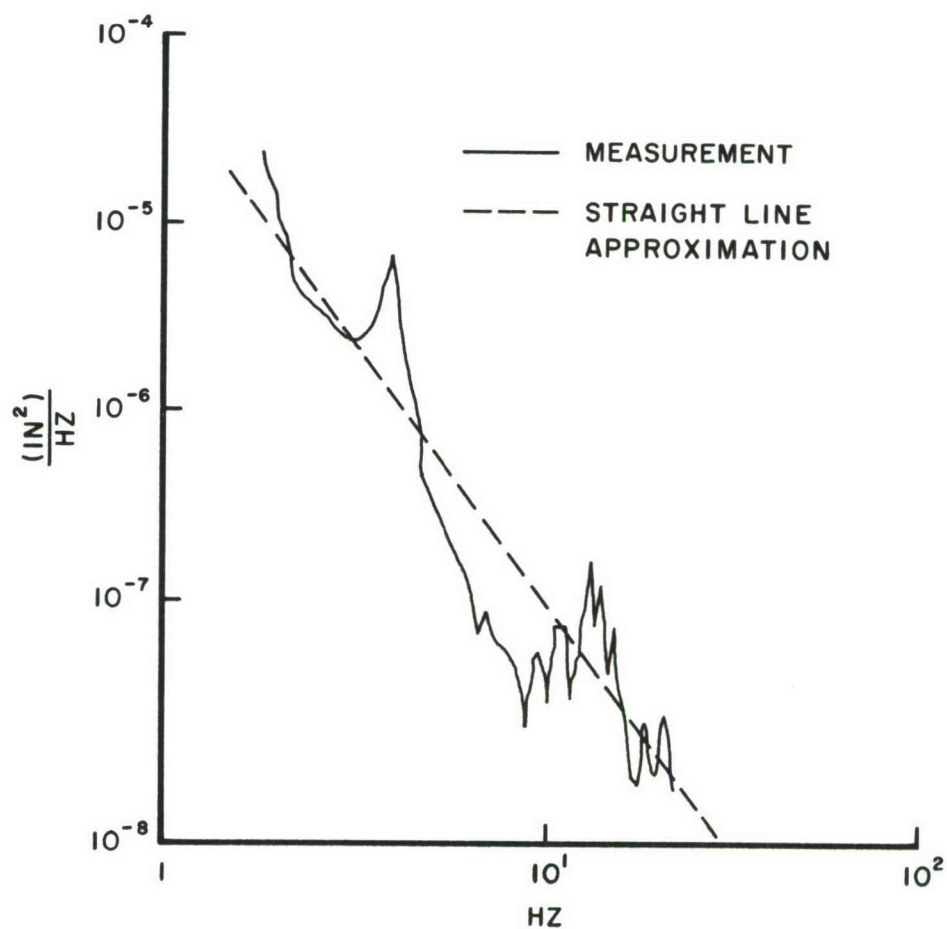


Figure 2. PSD of Transverse Vibration

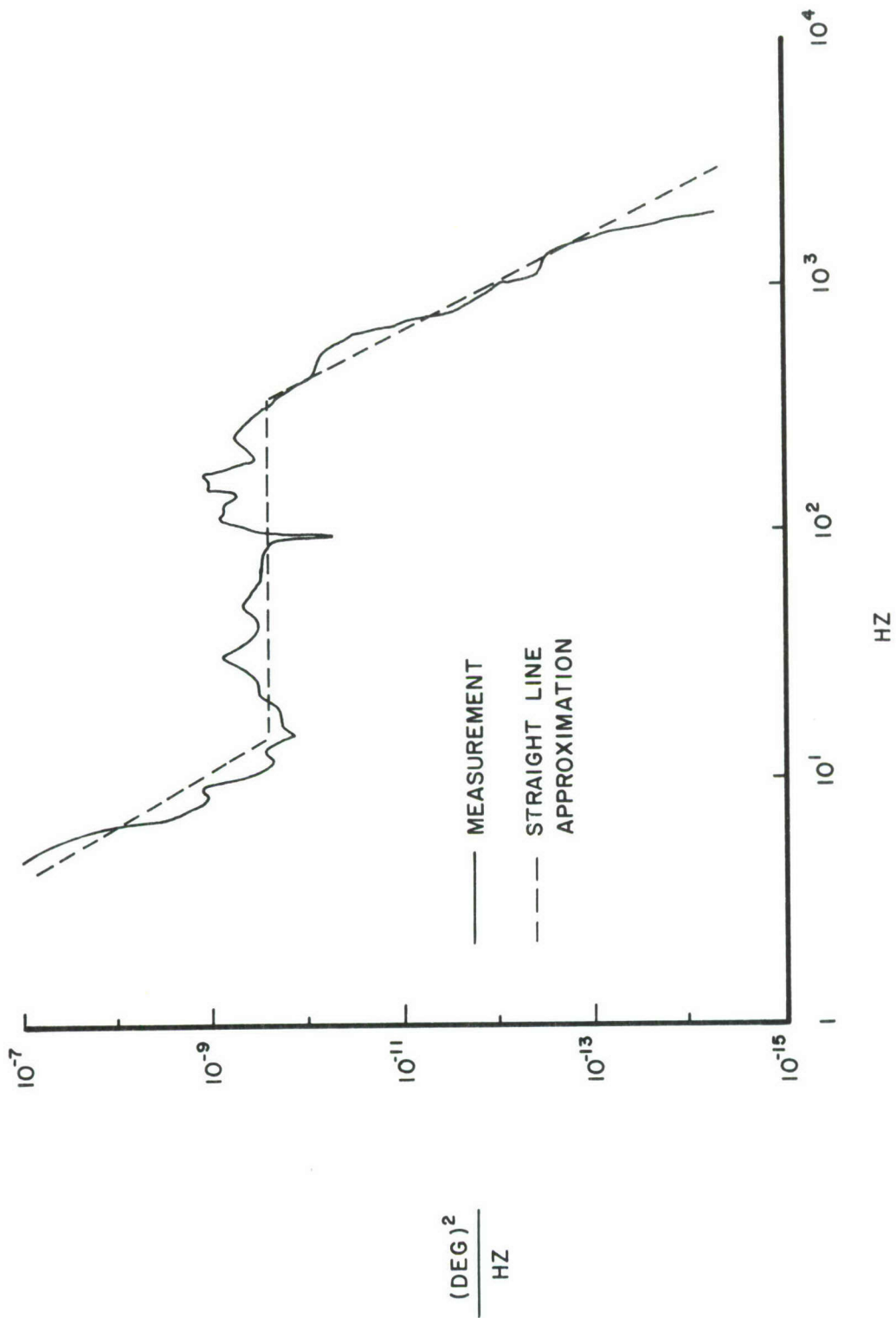


Figure 3. PSD of Angular Vibration

SECTION IV

THE DISCRETE ANGLE

Conventional transducer technology does not permit a direct measurement of angular vibration over a wide range of frequencies. In practice, the angle is approximated by differencing two linear transducer signals and dividing by the separation distance. That is, the discrete angle is defined by

$$\frac{\Delta y}{\Delta x} = \frac{y(x_1, t) - y(x_2, t)}{\Delta x}, \quad (28)$$

where $\Delta x = x_1 - x_2$. The discrete angle will approach the true angle $\theta(x, t)$ as $\Delta x \rightarrow 0$. In the actual measurement, Δx is anything but infinitesimal, hence Equation 28 is a working definition of a measurable angle rather than a limiting process to the true angle.

By repeating the stochastic dynamic analysis of Section II, the variance of $(\Delta y/\Delta x)$ can readily be computed and its first-term truncation is

$$\left\langle \left(\frac{\Delta y(x_1, x_2)}{\Delta x} \right)^2 \right\rangle = \left(\frac{\sin\left(\frac{\pi x_1}{L}\right) - \sin\left(\frac{\pi x_2}{L}\right)}{\Delta x} \right)^2 K I_{11} \quad (29)$$

With the use of the transformation $x_1 = x + \Delta x/2$ and $x_2 = x - \Delta x/2$, one has $\sin(\pi x_1/L) - \sin(\pi x_2/L) = 2 \cos(\pi x/L) \sin(\pi \Delta x/2L)$, hence

$$\left\langle \left(\frac{\Delta y(x)}{\Delta x} \right)^2 \right\rangle = \left(\frac{2 \sin\left(\frac{\pi \Delta x}{2L}\right)}{\Delta x} \right)^2 \cos^2\left(\frac{\pi x}{L}\right) K I_{11}. \quad (30)$$

Again, averaging Equation 30 over the beam, the beam-averaged rms of the discrete angle, $(\Delta y/\Delta x)_{\text{rms}} = \sqrt{L^{-1} \int_0^L \langle (\Delta y(x)/\Delta x)^2 \rangle dx}$, has the following

form similar to Equations 25 and 26

$$\left(\frac{\Delta y}{\Delta x}\right)_{\text{rms}} = \left(\frac{2 \sin\left(\frac{\pi \Delta x}{2L}\right)}{\Delta x}\right) \sqrt{\frac{K I_{11}}{2}}. \quad (31)$$

Since $(2 \sin(\pi \Delta x / 2L) / \Delta x) = \pi / L$ as $\Delta x \rightarrow 0$, it is seen that Equation 31 reduces to Equation 26 with the factor $\left(\sum_{n=1}^3 1/n^2\right)^{1/2}$ replaced by unity. The combination of Equations 25 and 31 would then yield a relationship between the linear and discrete angular rms of vibration amplitudes

$$\left(\frac{\Delta y}{\Delta x}\right)_{\text{rms}} = \frac{2 \sin\left(\frac{\pi \Delta x}{2L}\right)}{\Delta x} y_{\text{rms}}. \quad (32)$$

As pointed out before, the factor $(2 \sin(\pi \Delta x / 2L) / \Delta x)$ has the value (π / L) in the limit as $\Delta x \rightarrow 0$. In the other extreme case of $\Delta x = L$, however, it has the value $(2/L)$. Note that this factor varies almost 57% between the two extreme cases. In practice, the separation distance is neither infinitesimal nor the entire L ; let us therefore choose $\Delta x = L/2$, for which $(2 \sin(\pi \Delta x / 2L) / \Delta x)$ has the value $(2\sqrt{2}/L)$. In terms of the Δx , Equation 32 then becomes

$$\left(\frac{\Delta y}{\Delta x}\right)_{\text{rms}} = \frac{\sqrt{2}}{\Delta x} y_{\text{rms}}. \quad (33)$$

This is a counterpart of Equation 27 for the discrete angle case. The difference, however, is that Equation 33 refers to the separation distance Δx and not the beam length L . Like Equation 27, the relation shown in Equation 33 does not depend on the particular shape of normal modes; the details of spatial characterization have been eliminated by the beam averaging. In this respect, Equation 33 is an overall description of beam vibration in terms of the primary mode, which may qualitatively be valid regardless of the end condition.

Davis and Guckian (Reference 10) have reported some measurement of $(\Delta y / \Delta x)$ on a 156" x 60" x 30" bench plate externally excited to

simulate flight conditions. They have presented both the linear and angular vibration data in terms of the transfer-function magnitude. Unfortunately, they did not report the linear vibration data of the accelerometers from which the angular deflection was derived. It is therefore necessary to pick out linear vibration data from their report in such a way that the linear and angular vibration data would have the closest correspondence. For the angular vibration data given in Figures 54 through 57 of their report, the linear transfer-function magnitudes of their Figures 33 and 35 were chosen as the matching linear vibration data. To estimate the rms of fluctuations from a transfer-function magnitude, the following procedure has been adopted; (i) Assume a forcing psd of the form $C\omega^{-2}$ (C being a constant), (ii) approximate the transfer-function magnitude by a piecewise power formula, similar to approximating the psd by a power formula in Section III, (iii) multiply the squared transfer-function magnitude by the forcing psd, and (iv) integrate over the appropriate frequency range. For each of the angular vibration data, the measured $(\Delta y/\Delta x)_{\text{rms}}$ is estimated by the above procedure and compared with the predicted value based on Equation 33, as summarized in Table 2.

Discounting the case of Roll #2 whose measurement is apparently contaminated, one can predict by Equation 33 the measured angular rms within less than $\pm 20\%$. Although this is a fairly wide latitude, it must be remembered that the comparison of Table 2 is subject to several limitations. First of all, the prediction scheme (Equation 33) is valid only qualitatively; that it can work so satisfactorily is indeed a pleasant surprise. Second, the sets of linear and angular vibration data do not match exactly with respect to the transducer locations. Finally, the values of y_{rms} and $(\Delta y/\Delta x)_{\text{rms}}$ estimated from the transfer-function magnitude data are only approximate.

TABLE 2

COMPARISON OF THE MEASURED AND PREDICTED $(\Delta y/\Delta x)_{rms}$

Case	Measured	Measured		Δx (in)	Predicted $C^{-1/2} (\Delta y/\Delta x)_{rms}$	Deviation + (+ %)
	$C^{-1/2} (\Delta y/\Delta x)_{rms}$ (rad)	$C^{-1/2} y_{rms}$ (in)	Based on *			
Roll #1	7.28×10^{-3} Fig. 54	3.79×10^{-2} Fig. 35		6.25	8.58×10^{-3}	-15.2
Pitch #1	5.71×10^{-3} Fig. 55			9.0	5.96×10^{-3}	-4.2
Roll #2	1.8×10^{-2} Fig. 56	3.16×10^{-2} Fig. 33		6.25	7.15×10^{-3}	+151.7
Pitch #2	5.83×10^{-3} Fig. 57			9.0	4.97×10^{-3}	+18.1

Notes:

* Taken from the report of Davis and Guckian (Reference 10).

+ Deviation = $[\text{Measured } (\Delta y/\Delta x)_{rms} - \text{Predicted } (\Delta y/\Delta x)_{rms}] / \text{Predicted } (\Delta y/\Delta x)_{rms}$.

SECTION V

PRACTICAL DEFINITION OF THE DISCRETE ANGULAR VIBRATION

According to Equation 28, the direct measurement of $\langle (\Delta y / \Delta x)^2 \rangle$ involves taking the difference of the signals of two accelerometers which are separated by a predetermined distance Δx . In practice, the differencing of random signals is not a reliable operation because it tends to accentuate the noise part of random signals. Clearly, the smaller the separation distance the more acute the differencing error. An alternate definition will therefore be presented of the discrete angular vibration amplitude which involves subtraction of the well-behaved statistical averages and not the random signals themselves. To this end, square the right-hand side of Equation 28 and carry out the term-by-term averaging. The discrete angular variance is then expressed in terms of the linear variance $\langle y^2(x_i) \rangle$ and cross-correlation $\langle y(x_1) y(x_2) \rangle$

$$\left(\frac{\Delta y(x_1, x_2)}{\Delta x} \right)^2 = \frac{1}{(\Delta x)^2} \left[\langle y^2(x_1) \rangle + \langle y^2(x_2) \rangle - 2 \langle y(x_1) y(x_2) \rangle \right]. \quad (34)$$

Note that $\langle y^2(x_i) \rangle$ and $\langle y(x_1) y(x_2) \rangle$ are respectively the diagonal and off-diagonal elements of the covariance matrix $\langle y(x_i) y(x_j) \rangle$ ($i, j = 1, 2$). Hence, in terms of the covariance matrix, Equation 34 is a practical prescription for computing $\langle (\Delta y / \Delta x)^2 \rangle$, especially, when Δx is small.

Although the variance was computed in Section II, the cross-correlation has not yet been discussed. For the simply supported Bernoulli-Euler beam, $\langle y(x_1) y(x_2) \rangle$ can be written down immediately by replacing one of the $y(x)$'s in Equation 21a by $y(x_1)$ and the other $y(x)$ by $y(x_2)$

$$\langle y(x_1) y(x_2) \rangle = \sum_{n=1}^{\infty} \sin \left(\frac{n\pi x_1}{L} \right) \sin \left(\frac{n\pi x_2}{L} \right) K I_{nn}. \quad (35)$$

With the use of $x_1 = x + \Delta x/2$ and $x_2 = x - \Delta x/2$, Equation 35 becomes

$$\langle y(x_1) y(x_2) \rangle = \sum_{n=1}^{\infty} \left[\cos^2 \left(\frac{n\pi\Delta x}{2L} \right) - \cos^2 \left(\frac{n\pi x}{L} \right) \right] K I_{nn}. \quad (36)$$

As a consistency check, the insertion of Equation 36 together with the corresponding $\langle y^2(x_1) \rangle$ into Equation 34 reproduces the previously defined angular vibration amplitude, the leading term of which is Equation 30. This shows that Equation 34 is just another definition in terms of the covariance matrix. Recall that the assumption of the infinitely sharp forcing correlation, $\langle q(x_1)q(x_2) \rangle \sim \delta(x_1 - x_2)$, has been invoked in Section II-3. Therefore, one might suspect that $\langle y(x_1)y(x_2) \rangle$ would be fairly sharp. This however, turns out to be a false speculation because of the structural rigidity, so that the spatial correlation extends over the entire beam. As a typical example, let us compute the cross-correlation about the midpoint of beam. Then, with the use of $I_{nn} = I_{11}/n^4$, Equation 36 takes the following form

$$\langle y(L/2 + \Delta x/2) y(L/2 - \Delta x/2) \rangle = [F - G] K I_{11}, \quad (37)$$

$$\text{where } F = \sum_{n=1}^{\text{odd}} \frac{1}{n^4} \cos^2 \left(\frac{n\pi\Delta x}{2L} \right) \text{ and } G = \sum_{n=2}^{\text{even}} \frac{1}{n^4} \sin^2 \left(\frac{n\pi\Delta x}{2L} \right).$$

The square bracket of Equation 37 has the peak value at $\Delta x = 0$, and falls off to zero at the maximum separation $\Delta x = L$. It is, however, more meaningful to examine the correlation coefficient,

$$\eta = \frac{\langle y(L/2 + \Delta x/2) y(L/2 - \Delta x/2) \rangle}{\sqrt{\langle y^2(L/2 + \Delta x/2) \rangle} \sqrt{\langle y^2(L/2 - \Delta x/2) \rangle}},$$

which becomes

$$\eta = \frac{F - G}{F + G}. \quad (38)$$

Since F and G are always positive, it follows that $\eta \leq 1$; the equality is valid only when $\Delta x = 0$. The limiting value at $\Delta x = L$ cannot be deduced directly from Equation 38, for there it is indeterminate. However, it is found by the asymptotic analysis that $\eta = 1/2$ at $\Delta x = L$. The presence of spatial correlation over the entire beam is depicted in Figure 4.

In the remainder of this section, it will be shown that the prediction scheme in Equation 33 also follows from Equation 34, thus demonstrating consistency of that prediction. To the first-term truncation, the variance and cross-correlation are

$$\begin{aligned} \langle y^2(x_1) \rangle &= \sin^2 \left[\frac{\pi}{L} \left(x \pm \frac{\Delta x}{2} \right) \right] K I_{11}, \\ \langle y(x_1) y(x_2) \rangle &= \left[\cos^2 \left(\frac{\pi \Delta x}{2L} \right) - \cos^2 \left(\frac{\pi x}{L} \right) \right] K I_{11}, \end{aligned} \quad (39)$$

where $\langle y^2(x_1) \rangle$ and $\langle y^2(x_2) \rangle$ take the positive and negative signs, respectively. Now, introduce Equation 39 into the right-hand side of Equation 34. After averaging over the beam, one obtains

$$(\Delta y / \Delta x)_{\text{rms}} = \frac{1}{\Delta x} \left[K I_{11} - \left(2 \cos^2 \left(\frac{\pi \Delta x}{2L} \right) - 1 \right) K I_{11} \right]^{\frac{1}{2}}. \quad (40)$$

By identifying $K I_{11}$ with $2y_{\text{rms}}^2$, it is evident that $(2 \cos^2(\pi \Delta x / 2L) - 1)$ plays the role of a beam-averaged correlation coefficient. Further consolidation of Equation 40 by factoring out $K I_{11}$ ($= 2y_{\text{rms}}^2$) yields

$$(\Delta y / \Delta x)_{\text{rms}} = \frac{\sqrt{2} y_{\text{rms}}}{\Delta x} \sqrt{2 \left(1 - \cos^2 \left(\frac{\pi \Delta x}{2L} \right) \right)}. \quad (41)$$

Since $2(1 - \cos^2(\pi \Delta x / 2L)) = 1$ for $\Delta x = L/2$, Equation 41 becomes identical to Equation 33, thereby establishing the internal consistency of Equation 33 by way of an alternate derivation.

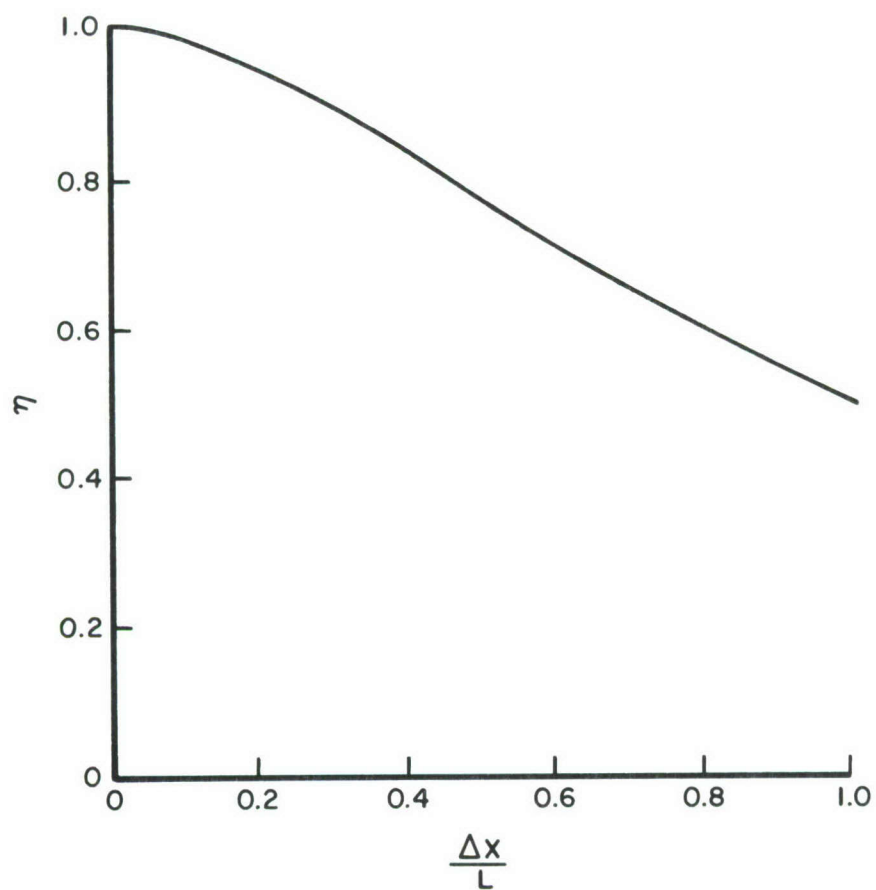


Figure 4. Correlation Coefficient

SECTION VI

CONCLUSIONS

By relating the linear and angular responses of structural vibration, qualitative relationships have been developed to predict the rms amplitude of angular vibration from a prescribed linear vibration response. The prediction schemes have been proposed for the true angular and discrete angular vibration amplitudes. Based on the presently available test data, the overall performance of predictions is within $\pm 20\%$ of the angular vibration measurement. Although crude, such a prediction capability is very satisfying. This is because the prediction schemes are intended for qualitative purposes and the present test data are limited only to gross confirmation. Since the present investigation is a first attempt, the refinement of angular vibration predictions will follow as more accurate vibration data become available.

APPENDIX

STOCHASTIC ANALYSIS OF THE TIMOSHENKO BEAM

For a small amplitude vibration, the angle of rotation may be approximated by $\partial y(x,t)/\partial x$; hence, the angular velocity and angular acceleration are $\partial^2 y/\partial x \partial t$ and $\partial^3 y/\partial x \partial t^2$, respectively. The Timoshenko beam equation which takes account of the angular damping and angular inertial effects, is given by

$$\frac{\partial^2 y}{\partial t^2} + 2\beta \frac{\partial y}{\partial t} + \frac{EI}{m} \frac{\partial^4 y}{\partial x^4} - 2\beta' \frac{\partial^3 y}{\partial x^2 \partial t} - \frac{I}{a} \frac{\partial^4 y}{\partial x^2 \partial t^2} = f(x,t). \quad (A1)$$

The last two terms of the left-hand side modify the Bernoulli-Euler beam Equation 1. Here β' is the appropriate damping constant, I is the moment of inertia, and a is the cross-section of beam. Although the angular inertial term, $-(I/a) \partial^4 y/\partial x^2 \partial t^2$, first appears in Rayleigh's classical beam equation (Reference 11), it is Timoshenko (Reference 1) who has investigated both the angular inertia and shearing deformation effects in the early 1920's; hence Equation A1 is referred to as a Timoshenko beam equation. More recently, Samuels and Eringen (Reference 12) have considered the most general Timoshenko beam equation in search for a convergent bending stress under purely random excitations.

For the simply supported case, the undamped normal modes of Equation A1 are still the same as the Bernoulli-Euler beam. Therefore, the stochastic analysis of Section II can be repeated verbatim by starting from the time-dependent equations

$$\alpha_n \ddot{y}_n + 2\gamma_n \dot{y}_n + \omega_n^2 y_n = q_n g(t),$$

where $\alpha_n = 1 + (I/a) (n\pi/L)^2$ and $\gamma_n = \beta + \beta' (n\pi/L)^2$ (Compare this with the Equation following Equations 2a and 2b in the main text). The linear and angular variances are again given by Equations 10 and 12, respectively, except for the modified I_{nk}

$$I_{nk} = \frac{1}{2} \int_{-\infty}^{\infty} F_g(\omega) H_n'(\omega) H_k'(\omega) d\omega, \quad (A2)$$

where $H'_n(\omega) = \frac{1}{\omega_n^2 + 2i\gamma_n\omega - \alpha_n\omega^2}$. Under the white-noise spectrum

(Equation 15), the evaluation of Equation A2 yields

$$I_{nk} = \frac{4\pi(\gamma_n/\alpha_n)F_0}{(\omega_n^2 - \omega_k^2 - 4\gamma_n^2/\alpha_n^2)^2 + (4\gamma_n/\alpha_n)^2(\omega_n^2\alpha_n - \gamma_n^2)},$$

which for $n = k$ simplifies to

$$I_{nn} = \frac{\pi F_0}{4\omega_n^2(\beta + \beta'(n\pi/L)^2)} \quad (A3)$$

Note that α_n does not appear in Equation A3; it is identical to Equation 17 if β is replaced by $\beta + \beta'(n\pi/L)^2$. The inclusion of angular effects has therefore resulted in more rapidly decreasing I_{nn} with respect to n , $I_{nn} \sim 1/n^6$; however, it has no effect on the prediction schemes derived in the main text.

REFERENCES

1. Timoshenko, S., Young, D. H., and Weaver, Jr., W., Vibration Problems in Engineering, 4th Ed. John Wiley & Sons, New York, 1974.
2. Eringen, A. C., "Response of Beams and Plates to Random Loads," Journal of Appl. Mech., Vol 24, 46 - 52, March 1957.
3. Bogdanoff, J. L. and Goldberg, J. E., "On the Bernoulli-Euler Beam Theory with Random Excitation," Journal of Aerospace Sci., Vol. 27, 371 - 376, May 1960.
4. Lyon, R. H., "Response of Strings to Random Noise Fields," Journal of Acoust. Soc. Am., Vol. 28, 391 - 398, May 1956.
5. Dyer, I., "Response of Plates to a Decaying and Convecting Random Pressure Field," Journal of Acoust. Soc. Am., Vol. 31, 922-928, July 1959.
6. Lin Y. K., Probabilistic Theory of Structural Dynamics, McGraw-Hill, New York, 1967.
7. Van Lear, G. A., Jr., and Uhlenbeck, G. E., "The Brownian Motion of Strings and Elastic Rods," Phys. Rev., Vol. 38, 1583 - 1598, November 1931.
8. Sher, L., Angular Vibration Effects on a Telescope System, AFWL-TR-72-202, AF Weapons Laboratory, Kirkland AFB, New Mexico, February 1973.
9. Davis, W. R., Jr., The Flight Induced Vibration of the Airborne Laser Laboratory Partial Aft Turret Fairing, AFFDL/FYS-75-3, AF Flight Dynamics Laboratory, Wright-Patterson AFB, Ohio, April 1975.
10. Davis, W. R., Jr., and Guckian, J. J., The Ground Vibration Survey of the Airborne Laser Laboratory (ALL) Cycle II Optical Bench, AFFDL/FYS-75-2, AF Flight Dynamics Laboratory, Wright-Patterson AFB, Ohio, April 1975.
11. Rayleigh, J. W. S., The Theory of Sound, Vol. 1, 2nd Ed. Dover, New York, 1945.
12. Samuels, J. C. and Eringen, A. C., "Response of a Simply Supported Timoshenko Beam to a Purely Random Gaussian Process," Journal of Appl. Mech., Vol. 25, 496 - 500, December 1958.